

Published in final edited form as:

Clin Chim Acta. 2010 January ; 411(1-2): 106–113. doi:10.1016/j.cca.2009.10.017.

A Novel Ultrasound-Based Method to Evaluate Hemostatic Function of Whole Blood

Francesco Viola¹, F. William Mauldin Jr.¹, Xiefan Lin-Schmidt¹, Doris M. Haverstick², Michael B. Lawrence¹, and William F. Walker^{1,3}

¹Department of Biomedical Engineering, University of Virginia, 415 Lane Rd. Charlottesville, VA 29908.

²Department of Pathology, University of Virginia, P.O. Box 800904, Charlottesville VA 22908

³Department of Electrical and Computer Engineering, University of Virginia, 351 McCormick Rd., Charlottesville VA 22904

Abstract

Background: Unregulated hemostasis represents a leading cause of mortality and morbidity in the developed world. Being able to recognize and quantify defects of the hemostatic process is critical to reduce mortality and implement appropriate treatment.

Methods: We describe a novel ultrasound-based technology, named sonorheometry, which can assess hemostasis function from a small sample of blood. Sonorheometry uses the phenomenon of acoustic radiation force to measure the dynamic changes in blood viscoelasticity during clot formation and clot dissolution. We performed *in vitro* experiments using whole blood samples of 1ml to demonstrate that sonorheometry is indicative of hemostatic functions that depend on plasma coagulation factors, platelets, and plasma fibrinolytic factors.

Results: Sonorheometry measurements show titration effects to compounds known to alter the coagulation factors (GPRP peptide, 0 to 8 mmol/l), platelets (abciximab, 0 to 12 ug/ml), and fibrinolytic factors (urokinase, 0 to 200U). Repeated measurements of blood samples from the same subjects yielded reproducibility errors on the order of 5%.

Conclusions: These data indicate that sonorheometry accurately quantifies the functional role of the components of hemostasis *in vitro*.

Keywords

hemostasis thrombosis and coagulation acoustic radiation force medical devices; point-of-care

1. Introduction

The formation of a blood clot and its successive dissolution, referred to as the hemostatic process, is required to arrest blood loss from an injured vessel. This process is the result of a

© 2009 Elsevier B.V. All rights reserved.

Corresponding Author: Francesco Viola, PhD, MR5, room 2117, 415 Lane Rd., Charlottesville, VA 22908. Phone: 434-924-9951, Fax: 434-982-3870, fv7d@virginia.edu.

Publisher's Disclaimer: This is a PDF file of an unedited manuscript that has been accepted for publication. As a service to our customers we are providing this early version of the manuscript. The manuscript will undergo copyediting, typesetting, and review of the resulting proof before it is published in its final citable form. Please note that during the production process errors may be discovered which could affect the content, and all legal disclaimers that apply to the journal pertain.

delicate functional balance between plasma coagulation factors, platelets, and fibrinolytic proteins. Each of these elements plays an important role in activating/deactivating the others, and the appropriate stimuli are necessary to prevent excessive blood loss without causing inappropriate thrombosis [1]. Disruption of this balance plays a significant role in the onset of potentially fatal conditions, including myocardial infarction, stroke, deep vein thrombosis, pulmonary embolism, and hemorrhage [2,3].

The hemostatic process is initiated by the activation and subsequent adhesion of platelets to the site of injury within the vessel wall. Activated platelets recruit other platelets and interact with fibrinogen in the blood plasma to form a platelet-plug that serves as the initial response to stop blood loss. Hemostasis then proceeds with a cascade of proteolytic reactions of the plasma coagulation proteins that ultimately form a three-dimensional network of fibrin that strengthens the platelet-plug. The fibrin chains are cross-linked and stabilized by the plasma factor XIIIa (FXIIIa). Platelets also have a central role in regulating the process of fibrin polymerization. The final step of hemostasis (ie, fibrinolysis) involves the activation of the plasma protein plasmin, which lyses the blood clot when its useful life is over. This cell-based model of hemostasis closely reflects the *in vivo* physiological process [4,5].

The mechanical properties of blood clots are essential for its primary function of stopping blood loss. Alterations in clot structure and its underlying mechanical properties have been implicated in thrombotic disease and other life threatening pathologies [6]. Recently, it was shown that fibrin clots of patients affected by premature coronary artery disease have a different structure and higher stiffness compared to the fibrin clots of healthy age-matched controls [7]. The mechanics of fibrin networks have been studied extensively at the macroscopic level [8,9]. The viscoelastic properties of individual fibrin strands have also been investigated by means of AFM [10] and “optical tweezers” [11]. Ferry et al. have initially investigated the viscoelastic properties of fibrin clots under small oscillating deformations [12-14]. These studies, however, have not examined the combined effects of coagulation plasma factors, platelets, and fibrinolytic proteins. Being able to monitor and characterize the mechanical properties of whole blood during clot formation and dissolution will (i) enhance understanding of both normal and pathological hemostasis, (ii) identify patients at high risk of bleeding and thrombotic disorders, (iii) inform appropriate medical treatment, and (iv) support the development of new pharmacological agents.

Current tests of hemostasis can be divided into two broad categories: endpoint biochemical assays and mechanical/viscoelastic analyzers. Endpoint assays are traditionally performed on blood plasma and include such tests as the pro-thrombin time (PT), activated partial thromboplastin time (aPTT), and the activated clotting time (ACT). While each of these assays measures a different aspect of the coagulation cascade, even in combination they do not provide a complete representation of overall hemostasis [15,16]. These tests are further limited by the absence of active platelets. In contrast, mechanical methods, such as the Thromboelastogram (TEG) and SonoClot, measure the contribution of all the components of hemostasis in whole blood. These methods have been widely studied and shown to offer valuable clinical and scientific insights [17]. However, they utilize complex and expensive mechanical transducers, resulting in instruments that are difficult to operate. In addition, the large mechanical strains (in the range of 8% to 16%) applied to the blood samples have been shown to interfere with clot formation and limit sensitivity and speed of the measurements [18,19].

We describe an ultrasound-based technology, named sonorheometry, which uses the phenomenon of acoustic radiation force to make repeated viscoelastic measurements of a whole blood sample [20]. We hypothesize that the dynamic changes of viscoelastic properties observed during clot formation and clot dissolution are representative of hemostatic function. In this paper, we present the results from controlled experiments showing that sonorheometry

can measure the function of plasma coagulation factors (including fibrinogen), platelets, and fibrinolytic factors from a small sample of whole blood.

2. Materials and Methods

2.1 Acoustic radiation force

Sonorheometry is performed using acoustic radiation force as a means to generate small and localized displacements within a blood sample. Returned echoes are processed to measure the induced displacements and determine viscoelastic properties of the sample. Acoustic radiation force results from the transfer of momentum that occurs when a propagating acoustic wave is either absorbed or reflected [21,22]. This body force acts in the direction of the propagating wave, and can be approximated by the following expression [22],

$$F = \frac{2\alpha \langle I(t) \rangle}{c} = \frac{2\alpha PII}{c} \frac{1}{\Delta T} \quad (1)$$

where α [m^{-1}] is the attenuation coefficient of the medium, c [m/s] is the speed of sound, $I(t)$ [W/m^2] is the instantaneous intensity of the ultrasound beam, PII is the pulse intensity integral, ΔT [s] is the time interval between successive ultrasound firings, and $\langle \rangle$ indicates a time averaged quantity. The pulse intensity integral is defined as the instantaneous intensity of a pulse integrated over the time where the acoustic pressure is nonzero.

Acoustic radiation force has been previously described as a method to characterize mechanical properties of soft tissues, including vitreous body, thyroid, and muscle [23,24].

2.2 Sonorheometry

For each measurement, a series of N ultrasound pulses are fired toward a specified location within the blood sample at time intervals ΔT (Fig. 1A). Each pulse generates radiation force as energy is absorbed and reflected during propagation. This radiation force induces displacements within the blood sample that depend upon local force application and mechanical properties of the blood. Each pulse also returns an echo as a portion of its energy is reflected from cell/plasma interfaces within the blood. Because the tissue moves slightly from one transmission to the next, the path length between the ultrasound transducer and any given region within the target changes with pulse number. This change in path length can be readily estimated from differences in the arrival times of echoes from the same region. The ensemble of these delays forms a time-displacement curve that describes the viscoelastic properties of the sample being analyzed (Fig. 1B). This process is then repeated M times, with intervening relaxation periods, to provide data about the dynamics of clot formation and dissolution.

As the blood rapidly changes from viscous fluid to viscoelastic solid during coagulation and then back to viscous fluid after clot lysis, we adaptively change the applied acoustic radiation force to induce displacements above the noise threshold, but below levels that could induce mechanical disruption. The magnitude of the force is adjusted to follow the changes in mechanical properties of the blood sample while keeping the strain below 3%, and thus within the linear range where elasticity is independent of strain amplitude [19]. Specifically, the maximum displacement induced during the $(m-1)^{\text{th}}$ acquisition is used to determine whether the force should be increased or decreased for the m^{th} acquisition, based on predetermined threshold values (with $m=1, \dots, M$). This adaptive process permits characterization of over five orders of magnitude in mechanical properties without generating high strain within the blood sample that could alter the underlying physiological processes. The values of the M maximum displacements are combined to form a relative compliance curve that is representative of the hemostatic process (Fig. 1C). We call this parameter “relative” since the absolute magnitude

of the radiation force is unknown due to its dependency on blood acoustic properties, which change throughout coagulation [25]. The curve shows characteristic features labeled TC_1 , TC_2 , CFR , S , TL_1 , and TL_2 . The parameter TC_1 corresponds to the rapid decrease in compliance observed in Fig. 1C. TC_1 is referred to as “time to clot” and is indicative of the beginning of fibrin polymerization. Similarly, the parameter TC_2 represents the ending of fibrin polymerization. The parameter CFR (clot formation rate) is the slope during fibrin polymerization and is indicative of the rate of fibrin polymerization. S (stiffness) is the minimum achieved compliance, corresponding to the maximum stiffness of the clot. This depends upon platelet function and the stiffness of the fibrin network. Finally, the times TL_1 and TL_2 can be defined to represent the initial and final phases of the fibrinolytic process and the consequent dissolution of the fibrin network (time to lysis). These parameters are summarized in Table 1.

2.3 Sonorheometry instrumentation

Sonorheometry has been implemented in a bench-top instrument (a photo of the instrument is available as Supplementary file). This prototype consists of a custom printed circuit board (PCB) controlled by an external laptop computer via USB 2.0 connection. The instrument supports two transmit and 4 receive ultrasound channels. The transmitter utilizes five-voltage levels and is composed of adjustable high voltage sources and high-speed transmitter drivers. Received echoes are amplified using a variable gain amplifier, band-pass filtered, and then digitized at 65MHz with 12-bit precision. The digitized data are then transferred to the adjacent laptop computer for data analysis. The transducer used in the experiments is a 10MHz piston transducer with a 1cm aperture, a 4cm fixed focus, and roughly 50% fractional bandwidth (Olympus NDT Inc., Waltham, MA). Acoustic radiation force is induced by applying ultrasound pulses (each 16 cycles long) at a PRF that is adaptively varied from 25Hz to 12.8KHz. Blood samples are analyzed using off the shelf polystyrene cuvettes (Fisher Scientific, Pittsburgh, PA). These cuvettes have low acoustic attenuation and acoustic impedance similar to that of blood; combined these properties allow us to deliver enough ultrasound signal within the blood to perform measurements. Sonorheometry measurements are performed every 6 seconds during coagulation and clot fibrinolysis. An off the shelf block heater (Fisher Scientific) and a custom-made water bath are used to hold the samples at body temperature while providing a propagation medium for the ultrasound beam.

2.4 Blood sampling and processing

The studies presented here were approved by the Investigational Review Board (IRB) of the University of Virginia. Blood samples were obtained from a peripheral vein of the arm into 6 1.8 ml Vacutainers™ (Becton Dickinson, Franklin Lakes, NJ) containing 3.2% (0.105 mol/l) sodium citrate to prevent coagulation within the tubes. The first tube was discarded, while the remaining tubes were placed on a rocker table and analyzed sequentially starting 30 min after the draw. For all the experiments described here, samples were obtained from a total of 8 volunteers (4 male and 4 female) with age range of 23-30 y (mean 25.75 ± 3.3 y) and with no history of thrombotic or hemorrhagic disorders.

In a typical experiment, 1 ml of citrated blood was pipette into a 4ml clear polystyrene cuvette along with 0.5 mg of kaolin activator to start coagulation through activation of the intrinsic pathway and 62 μ l of 0.2 mol/l $CaCl_2$ to reverse the anticoagulant effect of the sodium citrate. Other reagents were also added as required by the specific study performed. Phosphate buffer saline (PBS) solution was added to maintain identical blood dilution. Sonorheometry data acquisition was initiated exactly 1 min after all the reagents were pipetted into the sample, and measurements were performed every 6 sec.

2.5 Reagents

Gly-Pro-Arg-Pro (GPRP) was obtained from Calbiochem (EMD Chemicals Inc., Gibbstown, NJ) with 99.1% purity as determined by HPLC. It was dissolved in PBS into 100 mmol/l stock. Kaolin was obtained in powder form (Sigma Aldrich, St. Louis, MO) and suspended in sterile sodium chloride solution (Becton Dickinson, Franklin Lakes, NJ). Monoclonal antibody abciximab (ReoPro[®], Eli Lilly and Company, Indianapolis, IN) was obtained in a concentration of 2 mg/ml. The original solution was diluted by a factor of 5 by adding 200 μ L of PBS into 50 μ l of the original ReoPro solution. The serine protease abbo kinase (urokinase-type Plasminogen Activator, or uPA, Hyphen Biomed, Neuville-sur-Oise, France) was obtained in a concentration of 1 unit/ μ l.

2.6 Data analysis

The raw ultrasound data were transferred from the custom PCB to the laptop computer through USB interface and analyzed in MATLAB (Math Works Inc., Natick, MA). The data were first processed using a principal component filter to further remove noise and clutter due to reverberation and internal reflections within the cuvette [26]. Pulse-to-pulse time delays were estimated using a spline-based estimator [27] with a kernel of echo data of 1.2 mm and a search region of 57 μ m along the direction of propagation of ultrasound. The estimated delays were then assembled to generate time-displacement curves, similar to those depicted in Fig. 1B. From these curves we extrapolated the value of the maximum induced displacement, which were then normalized by their corresponding PRF and combined to form a relative compliance curve.

The sonorheometry parameters were calculated by fitting a sigmoidal curve and evaluating the first derivative of the curve, as shown in Figure 2. For example, the clotting times TC_1 and TC_2 were calculated based on a threshold value of the derivative curve (20% of the minimum value), whereas the clotting slope CFR is the minimum of the derivative curve. In the results presented here, the stiffness S was estimated using the value of the relative compliance 3 minutes after TC_2 . Identical methods and parameters were calculated for the fibrinolytic process.

Statistical analysis was performed in MATLAB. An unpaired, two-tailed *t*-test was used to assess the significance of the differences observed in sonorheometry parameters. In all instances, a $P < 0.05$ was considered significant.

3. Results

3.1 Assessment of coagulation plasma factors and fibrin polymerization

We performed experiments to characterize the function of the plasma coagulation factors and the consequent generation of a viscoelastic fibrin structure using sonorheometry. Fibrin is the building block of blood clots. Blood samples from 5 volunteers were obtained and the Gly-Pro-Arg-Pro (GPRP) peptide was added in titrated quantities to achieve final concentrations of 0, 1, 2, 4, and 8 mmol/l. GPRP is a strong inhibitor of fibrin polymerization that blocks the sites located in the γ chains at the two D end domains of the fibrinogen molecule [28]. Increasing concentrations of GPRP produced distinctive changes in mechanical properties, as shown in the sonorheometry compliance curve (Fig. 4). Figure 3A shows a set of typical sonorheometry curves obtained from a single volunteer. Both initial and final clotting times TC_1 and TC_2 increase with the concentration of GPRP [29,30]; significant changes are also observed for both the clot formation rate CFR and the stiffness S . As expected, the process of fibrin polymerization is a key component in determining the dynamics of clot formation and clot stiffness. Increasing levels of GPRP decreases both the rate of fibrin polymerization and the final stiffness of the formed clot.

3.2 Assessment of platelet function

Platelets play various important roles during hemostasis. These complex functions include: adhesion to the site of injury, activation and shape change, secretion of internal granules to recruit additional platelets, aggregation with surrounding platelets via fibrinogen links, interaction with fibrin mesh, and clot retraction in order to reduce the volume of the clot [31, 32]. Of particular importance is the mechanism of aggregation, which ultimately determines the ability to form a platelet plug that can stop bleeding. Aggregation is mediated by fibrinogen that binds to the glycoprotein (GP) IIb/IIIa, forming bridges between adjacent activated platelets. We performed experiments to investigate the contribution of platelets on sonorheometry measurements. Titrated quantities of monoclonal antibody abciximab were added to blood samples from 5 individuals to achieve final concentrations of 0, 2, 4, 6, 8, and 12 $\mu\text{g/ml}$. Abciximab is a potent inhibitor of platelet aggregation that prevents platelets from binding to fibrinogen by blocking the IIb/IIIa receptor on the platelet's surface [33,34]. The resulting sonorheometry curves demonstrate that increasing inhibition of platelet aggregation reduces the compliance S , yielding a softer clot (Fig. 4). The other parameters describing the dynamics of clot formation and dissolution do not change significantly, but fall within the variability of our measurements. Final clot stiffness varies by over one order of magnitude across the concentrations used for this experiment.

3.3 Assessment of fibrinolytic proteins

We also performed experiments to assess fibrinolysis using sonorheometry. For this set of experiments, we added titrated amounts of urokinase type plasminogen activator, a serine protease that promotes dissolution of the fibrin network that forms the blood clot [35]. Total amounts of urokinase were 0, 100, 150, and 200 U/ml of blood. Urokinase shows significant effects on the measurements performed by sonorheometry (Fig. 5), with the blood samples returning to a viscous fluid significantly faster with increasing concentrations of urokinase, as expected. Both clot lysis times TL_1 and TL_2 decrease as a function of urokinase concentration.

3.4 Reproducibility error of repeated sonorheometry measurements

The intrinsic variability of sonorheometry was tested using whole blood samples from 5 volunteers. For each subject, 10 samples were obtained into 1.8ml Vacutainers (with 3.2% sodium citrate) and analyzed sequentially using kaolin activation. The estimated CVs were <6% ($n=5$) for the all the parameters (the CV for LT_1 and LT_2 were not estimated since clot lysis was not observed within the experiment time of 15 mi).

3.5 Thermal and mechanical effects of sonorheometry

If not operated within specific limits, acoustic devices can produce significant tissue damage, including thermal and mechanical effects. Absorption of ultrasound signals through tissues leads to local heating, which might lead to thermal damage [36,37]. The mechanical effects of ultrasound are due primarily to cavitation, which involves the formation and rapid implosion (collapse) of a gas bubble [38]. The sudden collapse could results in mechanical damage.

We performed hydrophone measurements in de-ionized water (following the American Institute of Ultrasound in Medicine standards [39]) to quantify the acoustic output and the potential for adverse effects of sonorheometry. These experiments indicated that the maximum intensity generated by sonorheometry is on the order of 2.52 W/cm^2 (time average), which results in a maximum temperature increase of 0.01°C for each measurement [24,40]. Note that there is a 6 seconds interval between measurements, thus further limiting the overall temperature increase.

The hydrophone measurements also indicated that the potential for generating acoustic cavitation within the blood samples is greatly reduced and well within the Food and Drug Administration (FDA) limits set for general diagnostic ultrasound imaging (the calculated mechanical index is 0.26, over 7 times smaller than the FDA limit of 1.9) [36].

4. Discussion

While it is known that pathological alterations of the mechanical properties of blood clots are intimately related to thrombotic and hemorrhagic disease, it is essential to analyze every component of hemostasis and their interactions to fully characterize these properties. The balance between clotting factors, fibrin, platelets, and fibrinolytic proteins has great importance in determining the overall viscoelasticity of blood clots.

The results presented in this paper indicate that sonorheometry can quantify the dynamic changes in mechanical properties of whole blood during the process of coagulation and clot dissolution, and thus provides information about the relative contribution of the coagulation factors, platelets, and fibrinolytic proteins to overall hemostatic function. The activity of the coagulation proteins and the process of fibrin polymerization cause a rapid increase in clot stiffness, as shown by the reduced compliance in Figure 3. These results suggest that TC_1 and TC_2 are representative of the beginning and ending phases of fibrin polymerization caused by the coagulation factors in the plasma, whereas the slope CFR is representative of the rate of fibrin polymerization.

Figures 3 and 4 also suggest that the final stiffness of the clot results from the interaction of aggregated platelets and fibrin network. The parameter S is thus indicative of the combined mechanical functions of the fibrin network and the platelet aggregation/contractile function. The ability of sonorheometry to characterize platelet aggregation could be useful, for example, to determine the efficacy of therapies based on clopidogrel or non-steroidal anti-inflammatory drugs (NSAIDs) and to discriminate responders from non-responders to these drugs [41,42].

Figure 5 shows that the increased fibrinolytic activity caused by urokinase rapidly dissolves the blood clot and restores the original mechanical conditions prior to clot formation. The results in this figure suggest that the parameters TL_1 and TL_2 can be used to characterize dysfunctions of the fibrinolytic system, such as in the case of hyperfibrinolysis.

Sonorheometry requires neither moving mechanical parts nor direct contact with the sample and performs viscoelasticity measurements with minimal mechanical strain and without significant thermal and cavitation effects. The shear strains generated by the acoustic radiation force are kept below 3%, which is within the linear range of blood (the shear levels were also confirmed by computer simulations using finite element models). Furthermore, sonorheometry can be implemented with compact, readily available off-the-shelf electronic components. This potential for miniaturization will be critical in future work to develop an instrument that can be easily transported to the patient's bedside. The use of smaller blood samples, such as those that might be obtained through a finger-stick, could be achieved by increasing the center frequency of the ultrasound pulses used to generate acoustic radiation force. Higher frequencies not only reduce the dimensions of the ultrasound beam, but also increase attenuation within the blood sample, which increases the magnitude of the applied acoustic radiation force [43].

Sonorheometry holds great potential to improve patient diagnosis and treatment in a variety of clinical scenarios. By utilizing different activators, blocking agents, and other reagents, sonorheometry could provide a highly versatile platform for (i) screening for increased bleeding or clotting risks, (ii) guiding patient care in a variety of clinical settings, and (iii) discovering fundamental clotting/bleeding mechanisms. This is of great importance since thrombotic and hemorrhagic diseases represent the leading cause of mortality and morbidity

in the developed world [2]. One possible application for this technology could be to guide transfusions of blood products during emergency or surgical procedures [44-46]. While transfusions of blood products have had a significant impact in saving millions of lives, blood is a scarce resource and usage must be carefully optimized. Furthermore, several concerns still exist regarding the safety of transfusion therapies, which carry risks of infection and immune response. Current transfusion guidelines are rarely implemented in clinical practice due to the limitations of current technology. Because of these limitations, the clinical state of the art in most institutions is iterative transfusion and subjective evaluation of bleeding [46]. This process is slow and prone to over-transfusion. We envision sonorheometry to quantify the hemostatic system at the patient's bedside and inform targeted use of blood products, thus minimizing unnecessary transfusions, speeding treatment, and improving patient outcomes.

In conclusion, we introduced a novel technology and presented experimental results that showed the capability of this technology to assess the function of coagulation factors, platelets, and fibrinolytic proteins in whole blood. Future developments include the use of a second ultrasound transducer at the opposite end of the blood sample under analysis to estimate variation in acoustic properties through the sample. This will allow determining the absolute value of the viscoelastic parameters (rather than indirect relative parameters).

Supplementary Material

Refer to Web version on PubMed Central for supplementary material.

Acknowledgments

This work was supported by the National Institute of Health (NIH) grant EB005433 and by the Wallace H. Coulter Translational Partnership Award at the University of Virginia. We thank Dr. Thomas C. Skalak for his thoughtful critique of this manuscript.

References

1. Laposata, M., et al. The Clinical Hemostasis Handbook. Year Book Medical Publisher; 1989.
2. Hoyert DL, Kung HC, Smith BL. Deaths: preliminary data for 2003. *Natl Vital Stat Rep* 2005;53:1-48.
3. Hambleton J, Leung LL, Levi M. Coagulation: Consultative Hemostasis. *Hematology* 2002;1:335-352. [PubMed: 12446431]
4. Hoffman M, Monroe DM. A cell-based model of hemostasis. *Thromb Haemost* 2001;85:958-965. [PubMed: 11434702]
5. Becker RC. Cell-Based Models of Coagulation: A Paradigm in Evolution. *J Thromb Thrombolysis* 2005;20:65-68. [PubMed: 16133899]
6. Weisel JW. Enigmas of Blood Clot Elasticity. *Science* 2008;320:456. [PubMed: 18436761]
7. Collet J-P, Allali C, Lesty ML, et al. Altered Fibrin Architecture Is Associated With Hypofibrinolysis and premature Coronary Atherothrombosis. *Arterioscler Thromb Vasc Biol* 2006;26:2567-2573. [PubMed: 16917107]
8. Ryan EA, Mockros LF, Weisel JW, Lorand L. Structural Origins of Fibrin Clot Rheology. *Biophys J* 1999;77:2813-2826. [PubMed: 10545379]
9. Jen CJ, McIntire LV. The Structural Properties and Contractile Force of a Clot. *Cell Motil* 1982;2:445-455. [PubMed: 6891618]
10. Liu W, Jawerth LM, Sparks EA, et al. Fibrin Fibers Have Extraordinary Extensibility and Elasticity. *Science* 2006;313:634. [PubMed: 16888133]
11. Collet J-P, Shuman H, Ledger RE, Lee S, Weisel JW. The elasticity of an individual fibrin fiber in a clot. *Proc Natl Acad Sci USA* 2005;102:9133-9137. [PubMed: 15967976]
12. Roberts WW, Kramer O, Rosser RW, Nestler FHM, Ferry JD. Rheology of Fibrin Clots I. Dynamic Viscoelastic Properties and Fluid Permeation. *Biophys Chem* 1974;1:152-160. [PubMed: 4425722]

13. Gerth C, Roberts WW, Ferry JD. Rheology of Fibrin Clots II. Linear Viscoelastic Behavior in Shear Creep. *Biophys Chem* 1974;2:208–217. [PubMed: 4474029]
14. Nelb GW, Kamykowsky GW, Ferry JD. Rheology of Fibrin Clots V. Shear Modulus, Creep, and Creep Recovery of Fine Uligated Clots. *Biophys Chem* 1981;13:15–23. [PubMed: 7260325]
15. Gravlee GP, Arora S, Lavender SW, et al. Predictive value of blood clotting tests in cardiac surgical patients. *Ann Thorac Surg* 1994;58:216–221. [PubMed: 8037528]
16. Bajaj SP, Joist JH. New Insights into how blood clots: Implications for the use of APTT and PT as coagulation screening tests and in monitoring anticoagulant therapy. *Semin Thromb Hemost* 1999;25:407–418. [PubMed: 10548073]
17. Ganter MT, Hofer CK. Coagulation Monitoring: Current Techniques and Clinical Use of Viscoelastic Point-of-Care Coagulation Devices. *Anesth Analg* 2008;106:1366–1374. [PubMed: 18420846]
18. Evans PA, Hawkins K, Lawrence M, Williams RL, Barrow MS, Thirumalai N, Williams PR. Rheometry and associated techniques for blood coagulation studies. *Med Eng Phys* 2008;30:671–679. [PubMed: 17900965]
19. Burghardt WF, Goldstick TK, Leneschmidt J, Kempka K. Nonlinear viscoelasticity and thromboelastograph. 1. Studies on bovine plasma clots. *Biorheology* 1995;32:621–630. [PubMed: 8857352]
20. Viola F, Kramer MD, Lawrence MB, Oberhauser JP, Walker WF. Sonorheometry: A Non-contact Method for the Dynamic Assessment of Thrombosis. *Annals Biom Eng* 2004;32:696–705.
21. Torr GR. The Acoustic Radiation Force. *Am J Phys* 1984;52:402–408.
22. Starritt HC, Duck FA, Humphrey VF. Forces acting in the direction of propagation in pulsed ultrasound fields. *Phys Med Biol* 1991;36:1465–1474. [PubMed: 1754617]
23. Viola F, Walker WF. Radiation force Imaging of Viscoelastic Properties with Reduced Artifacts. *IEEE Trans on Ultrason Ferroelect and Freq Contr* 2003;50:736–742.
24. Nightingale KR, Soo MS, Nightingale RW, Trahey GE. Acoustic Radiation Force Impulse Imaging: In vivo Demonstration of Clinical Feasibility. *Ultrasound Med Biol* 2002;28:227–235. [PubMed: 11937286]
25. Shung KK, Fei D, Yuan Y, Reeves WC. Ultrasonic Characterization of Blood During Coagulation. *J Clin Ultrasound* 1984;12:147–153. [PubMed: 6423688]
26. Mauldin FW Jr, Viola F, Walker WF. Reduction of Echo Decorrelation Via Complex Principal Component Filtering. *Ultrasound Med Biol* 2009;35:1325–1343. [PubMed: 19520491]
27. Viola F, Walker WF. A Spline Based Algorithm for Continuous Time Delay Estimation Using Sampled Data. *IEEE Trans Ultrason Ferroelect Freq Cont* 2005;52:80–93.
28. Laudano AP, Doolittle RF. Studies on synthetic peptides that bind to fibrinogen and prevent fibrin polymerization. Structural requirements, number of binding sites, and species differences. *Biochem* 1980;19:1013–1019. [PubMed: 7356959]
29. Chakroun T, Gerotziapas GT, Seghatchian J, et al. The influence of fibrin polymerization and platelet-mediated contractile forces on citrated whole blood thromboelastography profile. *Thromb Haemost* 2006;95:822–828. [PubMed: 16676074]
30. Laudano AP, Doolittle RF. Synthetic peptide derivatives that bind to fibrinogen and prevent the polymerization of fibrin monomers. *Proc Natl Acad Sci USA* 1978;75:3085–3089. [PubMed: 277910]
31. Carr ME. In Vitro Assessment of Platelet Function. *Trans Med Review* 1997;11:106–115.
32. Packham MA. Role of platelets in thrombosis and hemostasis. *Can J Physiol Pharmacol* 1994;72:278–284. [PubMed: 8069774]
33. The EPIC Investigators. Use of monoclonal antibody directed against the platelet glycoprotein IIb/IIIa receptor in high-risk coronary angioplasty. *N Engl J Med* 1994;330:956–961. [PubMed: 8121459]
34. Collier BS, Peerschke EI, Scudder LE, Sullivan CA. A murine monoclonal antibody that completely blocks the binding of fibrinogen to platelets produces a thrombasthenic-like state in normal platelets and binds to glycoproteins IIb and/or IIIa. *J Clin Invest* 1983;72:325–338. [PubMed: 6308050]

35. Lijnen HR, VanHoef B, DeCock F, Collen D. The mechanism of plasminogen activation and fibrin dissolution by single chain urokinase-type plasminogen activator in a plasma milieu in vitro. *Blood* 1989;73:1864–1872. [PubMed: 2713507]
36. American Institute of Ultrasound in Medicine. Bioeffects and Safety of Diagnostic Ultrasound. 1993
37. NCRP Report No. 113. Exposure Criteria for Medical Diagnostic Ultrasound: I. Criteria Based on Thermal Mechanisms. NCRP Publications; 1992.
38. Apfel RE, Holland CK. Gauging the likelihood of cavitation from short-pulse, low-duty cycle diagnostic ultrasound. *Ultrasound Med Biol* 1991;17:179–185. [PubMed: 2053214]
39. American Institute of Ultrasound in Medicine. Acoustic Output Measurement and Standard for Diagnostic Ultrasound Equipment. 1998
40. Palmeri ML, Nightingale K. On the Thermal Effects Associated with Radiation Force Imaging of Soft Tissue. *IEEE Trans Ultrason Ferroelect Freq Cont* 2004;51:551–565.
41. Michelson AD. Platelet function testing in cardiovascular diseases. *Circulation* 2004;110:e489–493. [PubMed: 15533872]
42. Cattaneo M. Aspirin and clopidogrel: efficacy, safety, and the issue of drug resistance. *Arterioscler Thromb Vasc Biol* 2004;24:1980–1987. [PubMed: 15388526]
43. Szabo, TL. Diagnostic Ultrasound Imaging. Academy Press; 2004.
44. Snyder-Ramos SA, Mohnle P, et al. The ongoing variability in blood transfusion practices in cardiac surgery. *Transfusion* 2008;48:1284–1299. [PubMed: 18422857]
45. Avidan MS, Alcock EL, et al. Comparison of structured use of routine laboratory tests or near-patient assessment with clinical judgment in the management of bleeding after cardiac surgery. *BJA* 2004;92:178–186. [PubMed: 14722166]
46. Ferraris VA, Ferraris SP, Saha SP, et al. Perioperative blood transfusion and blood conservation in cardiac surgery: the Society of Thoracic Surgeons and The Society of Cardiovascular Anesthesiologists clinical practice guidelines. *Ann Thorac Surg* 2007;83:S27–S86. [PubMed: 17462454]

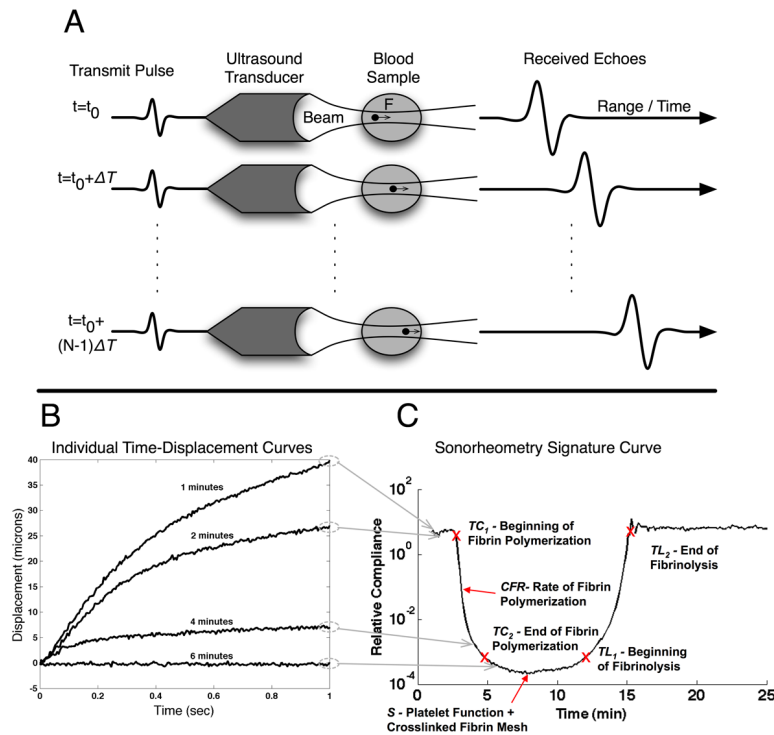


Figure 1.

Overview of sonorheometry. (A) A series of N acoustic pulses are sent into the blood sample at a specified pulse repetition frequency (PRF). These pulses generate acoustic radiation force that induces a deformation field within the sample. The deformation field can be estimated from the time delays of the N returning echoes. (B) Typical displacement curves generated within the blood sample. As blood coagulates we observe reduced displacement. (C) Maximum displacements are combined to form graphs of relative compliance, which characterize the overall hemostatic process. The parameter TC_1 corresponds to the time of initial decrease in relative compliance and represents the beginning of fibrin polymerization. The parameter TC_2 occurs at the time of maximum fibrin polymerization. The parameter CFR corresponds to the slope during fibrin polymerization and it is indicative of the rate of fibrin polymerization. S represents the minimum compliance (or maximum stiffness of the clot), which depends upon platelet function and the stiffness of the fibrin network. Finally, TL_1 is indicative of the start of the fibrinolytic process and the corresponding dissolution of the fibrin network. Similarly, TL_2 time can be defined to indicate the end of fibrinolysis.

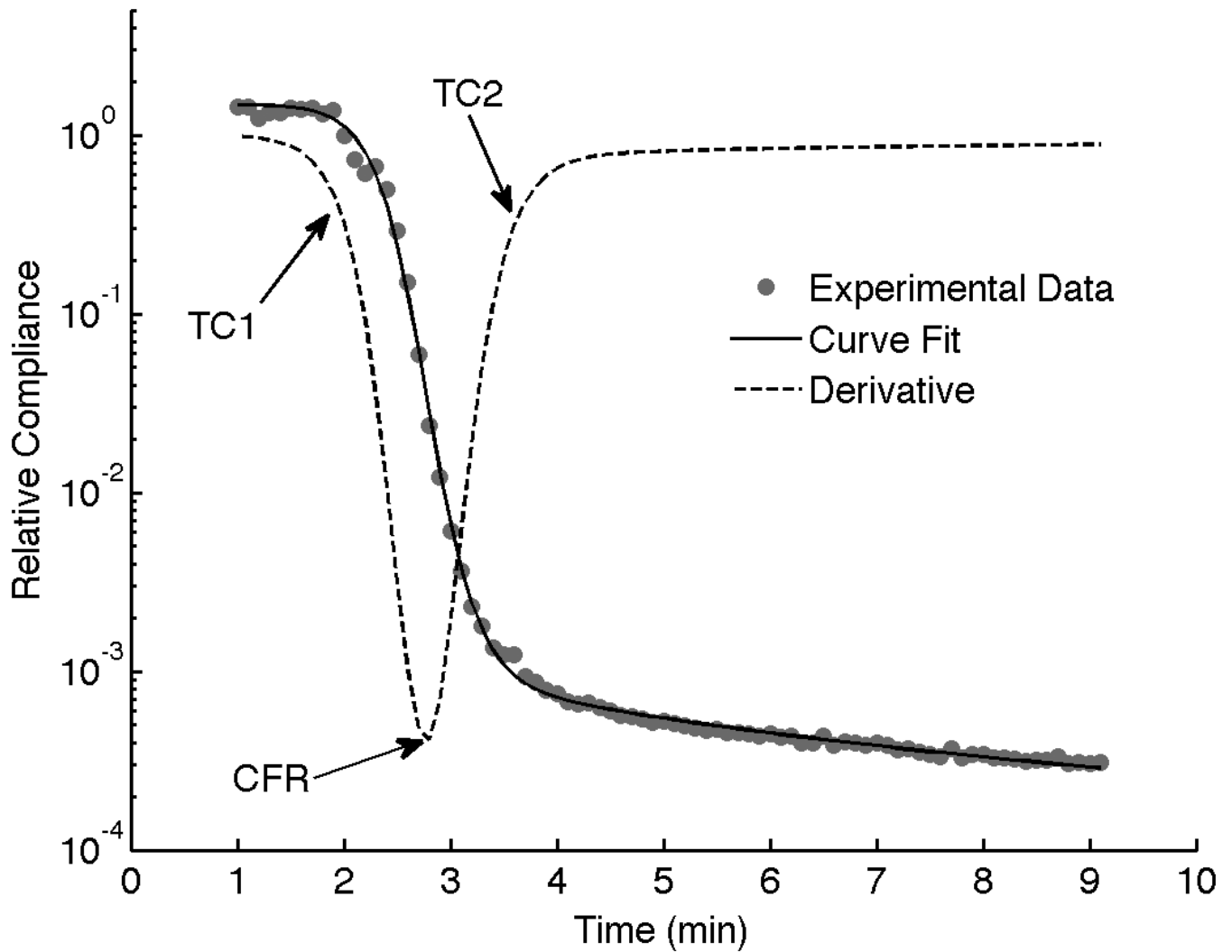
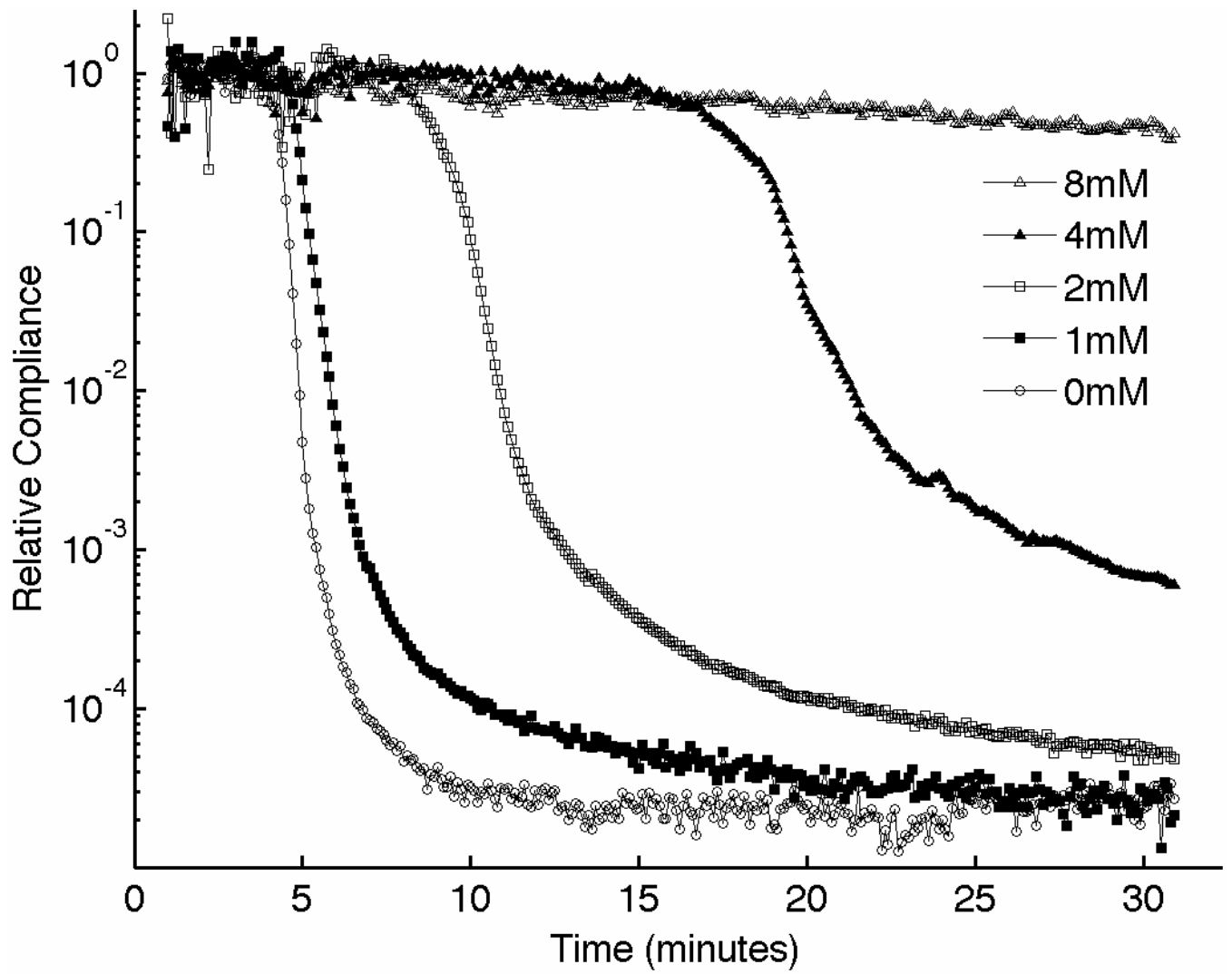
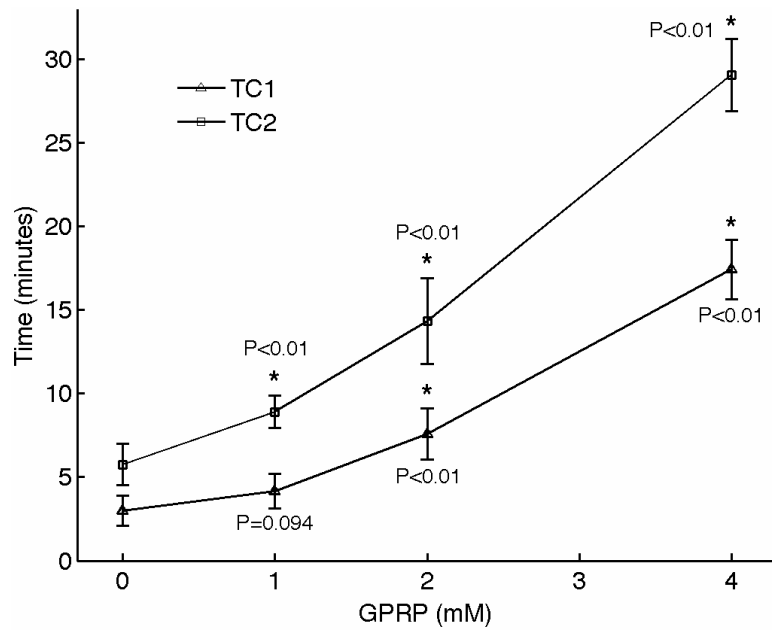


Figure 2.

The characteristic parameters output by sonorheometry are obtained by performing a non-linear curve fit of the experimental data and obtaining the first derivative of the model curve as a function of time. Clotting times TC_1 and TC_2 are calculated based on a threshold value of the derivative curve (20% of the minimum value). The clotting slope CFR is the minimum of the derivative curve. The minimum compliance S represents the maximum stiffness of the formed blood clot. Identical parameters can be calculated for the fibrinolytic process (not shown in this figure).





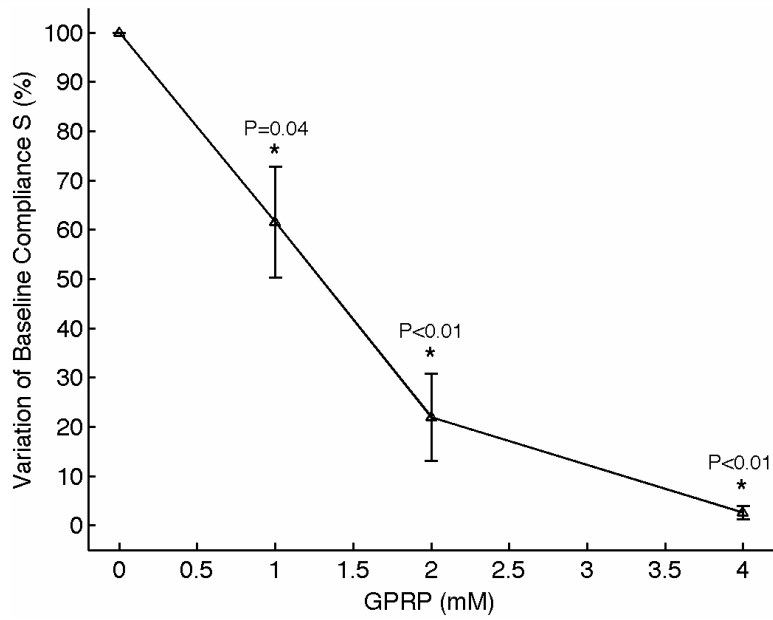
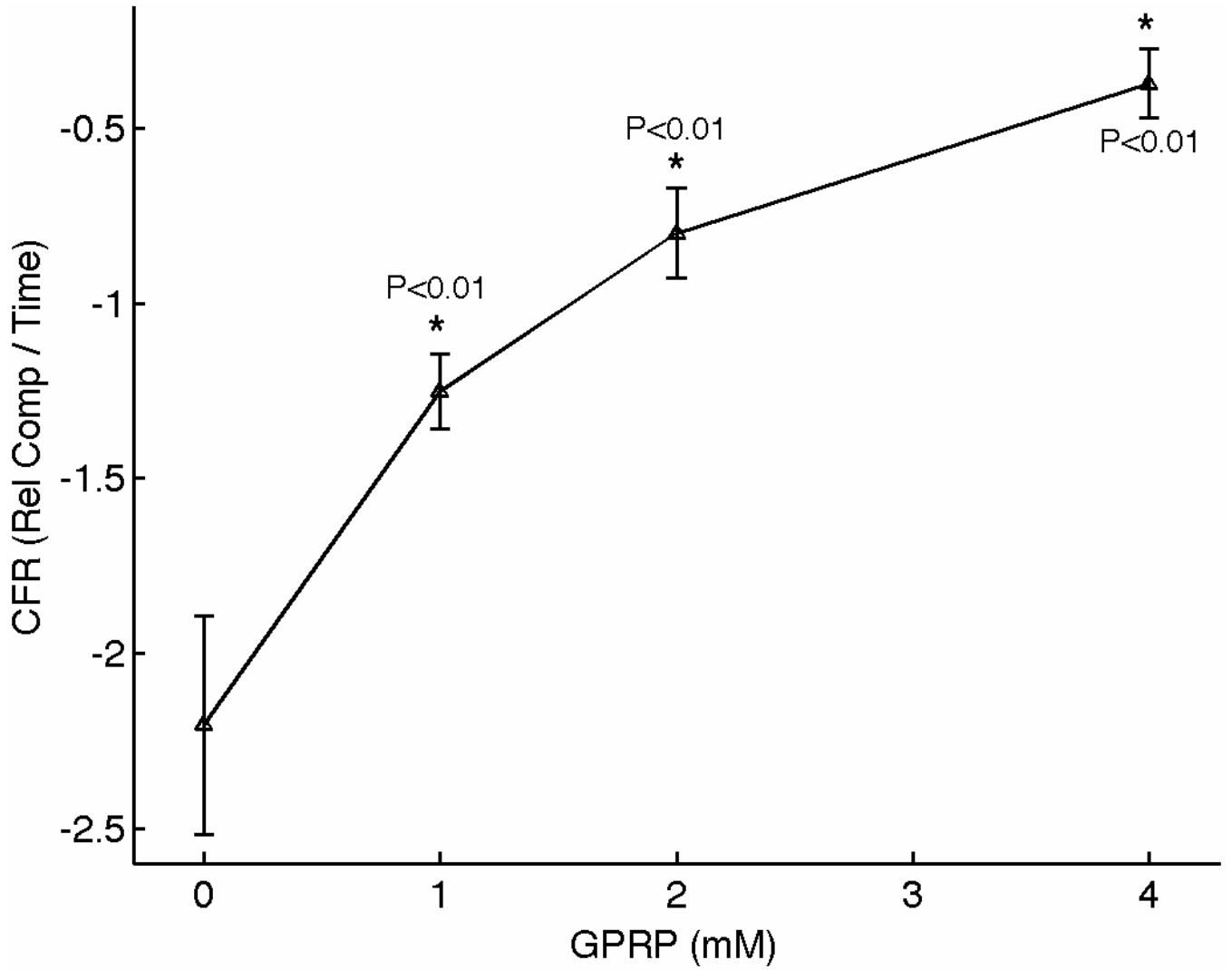
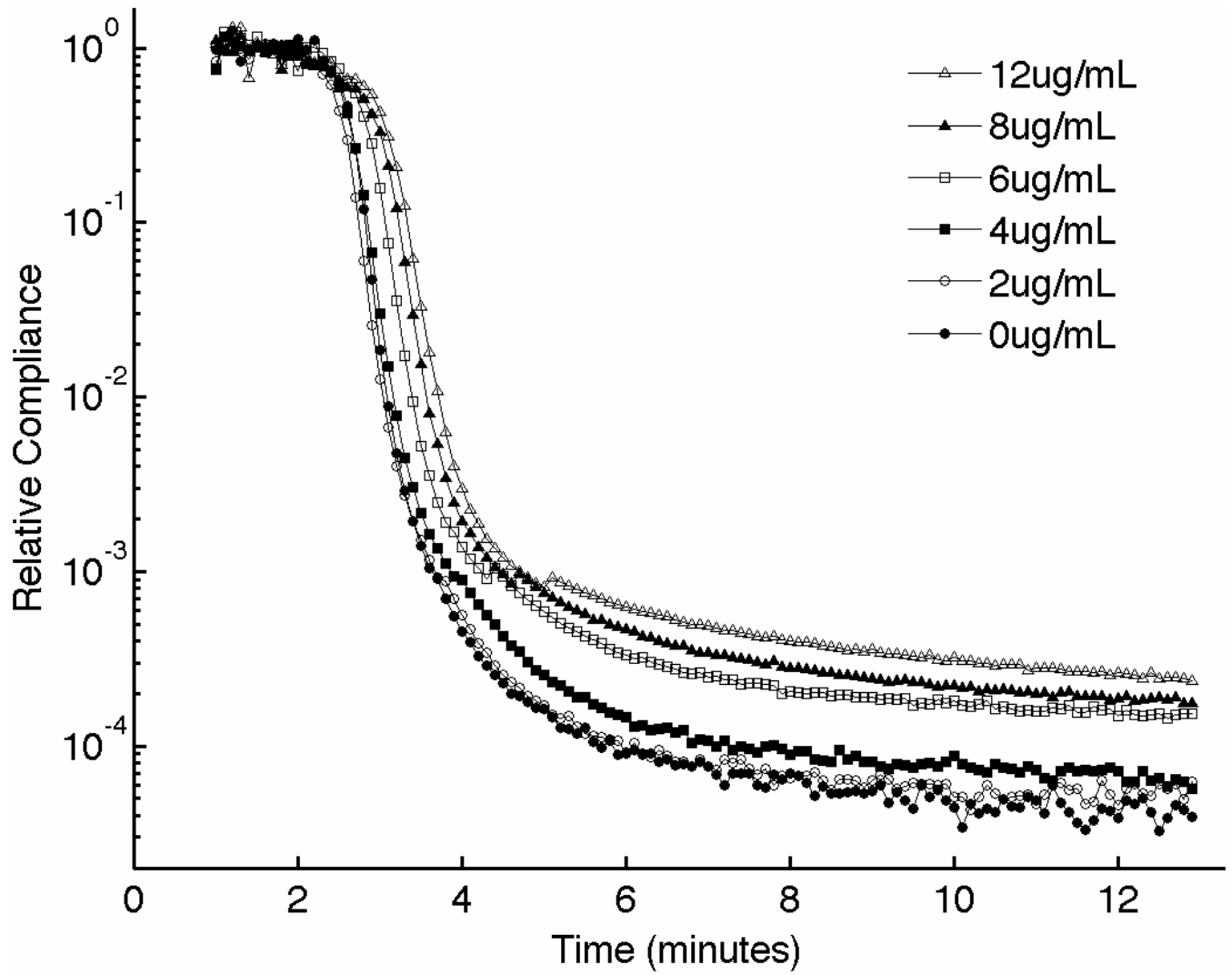


Figure 3.

(A) Representative sonorheometry curves across GPRP concentrations ranging from 0 to 8mmol/l. The GPRP peptide inhibits fibrin polymerization, resulting in blood clots that form more slowly and with reduced stiffness. 8mmol/l GPRP resulted in lack of measurable changes in viscoelasticity of the samples. (B) The initial and final clotting times TC_1 and TC_2 increase significantly with GPRP concentration. (C) Significant variations are also observed for the slope CFR , indicating a reduction in the rate of fibrin polymerization. (D) The baseline compliance S is also affected by GPRP, which results in softer clots due to the reduced amount of fibrin (the sample with no GPRP was assumed as reference point). Error bars in each figure show one standard deviation; statistics were obtained over 5 normal subjects with no history of thrombotic or hemorrhagic disorders. Significance values (P-values) were calculated in comparison to the control with no GPRP. Although presented in percentages, statistical significance in panel (D) was assessed using the stiffness values.



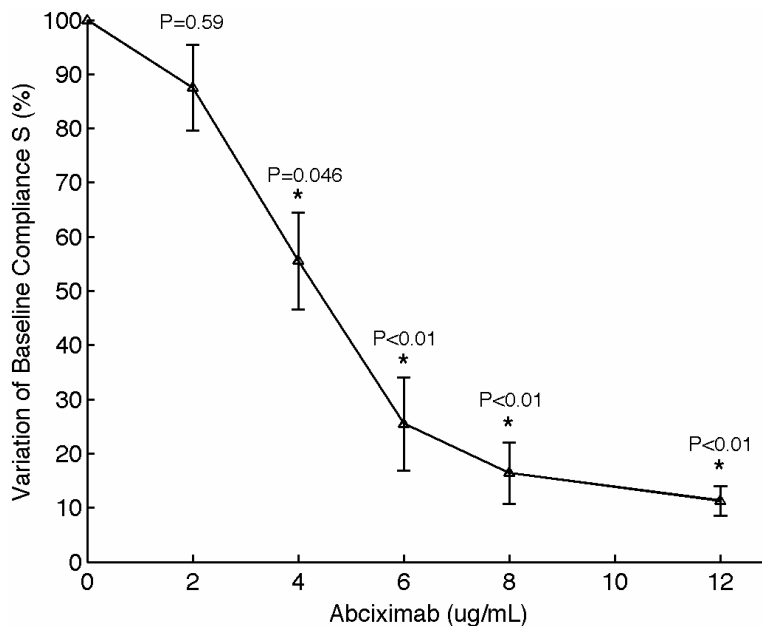


Figure 4.

(A) Representative sonorheometry curves as a function of abciximab concentration (from 0 to 12 $\mu\text{g/ml}$). The monoclonal antibody abciximab is a potent inhibitor of platelet-fibrinogen aggregation through the IIb/IIIa receptor. (B) The baseline compliance S diminishes with abciximab concentration due to decreased platelet aggregation (the sample with no abciximab was assumed as reference point). Error bars show one standard deviation; statistics were obtained over 5 normal subjects with no history of thrombotic or hemorrhagic disorders. Significance values (P-values) were calculated in comparison to the control with no abciximab. Although presented in percentages, statistical significance in panel (B) was assessed using the stiffness values.

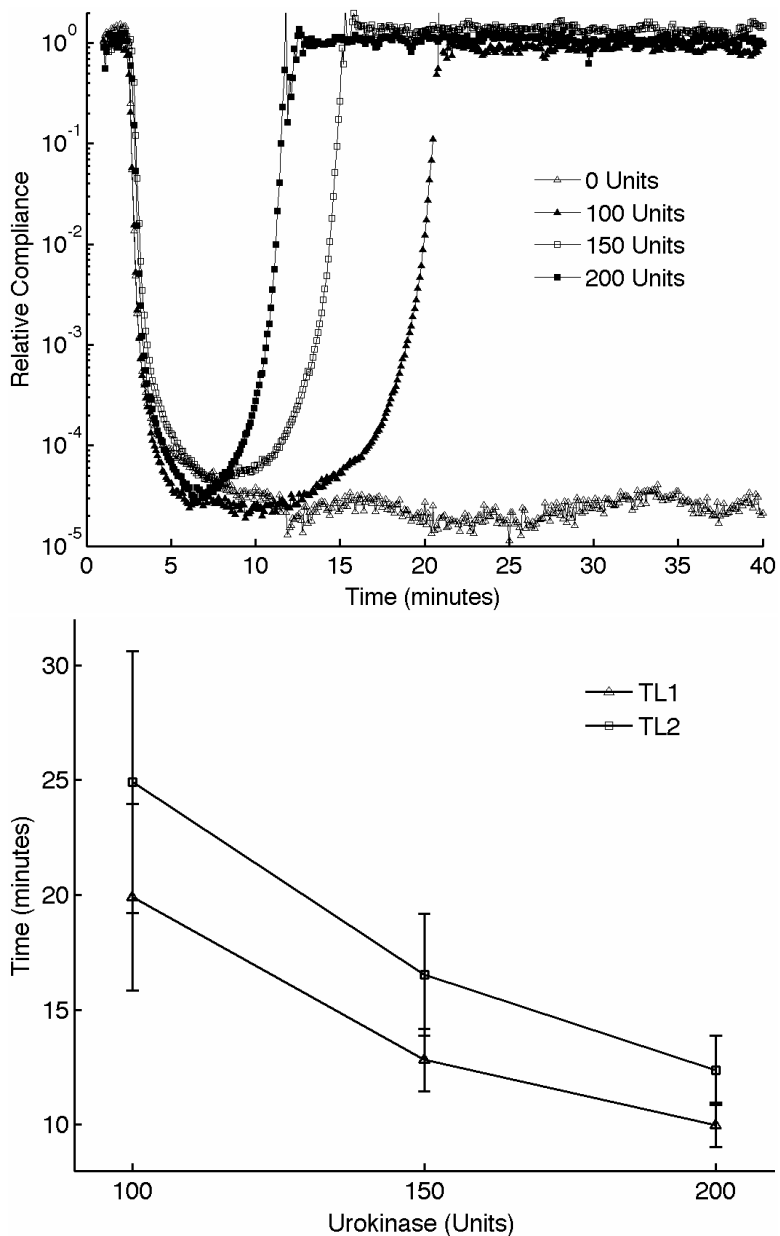


Figure 5.

(A) Representative sonorheometry curves in the presence of increasing concentration of urokinase type plasminogen activator, a serine protease that accelerates dissolution of the fibrin network. (B) Clot lysis occurs significantly faster as urokinase concentration is increased, as indicated by the clot lysing times TL_1 and TL_2 . Error bars show one standard deviation; statistics were obtained over 5 normal subjects with no history of thrombotic or hemorrhagic disorders. Since the samples with 0 units of urokinase did not show evidence of fibrinolysis, control values for TL_1 and TL_2 could not be estimated and statistical significance could not be rigorously assessed.

Table 1

Parameters output by sonorheometry and corresponding information provided.

Parameter	Information provided	Dependent upon
TC_1, TC_2	Measure initial and final fibrin formation	Function of fibrinogen and other plasma coagulation proteins
S	Fibrin and platelet activity	Combined effects of fibrin network and platelet aggregation
CFR	Rate fibrin polymerization	Function of fibrinogen and other plasma coagulation proteins
TL_1, TL_2	Clot dissolving process	Function of fibrinolytic proteins of the plasma